Galactic magnetic field (M51)

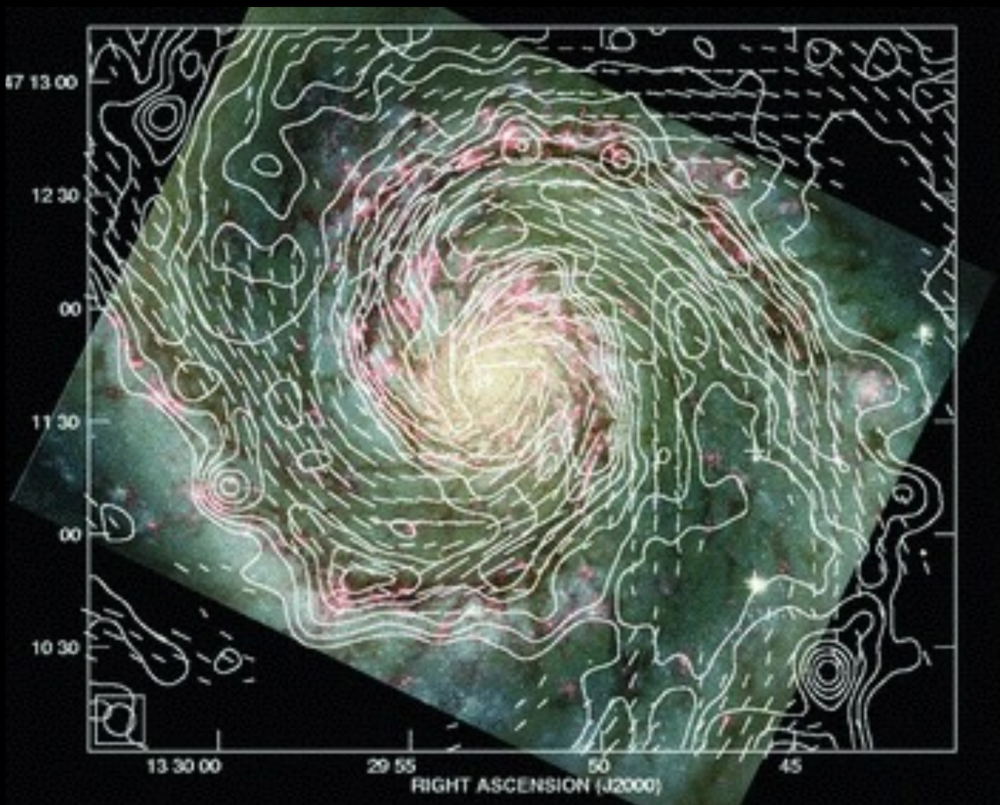

B-direction from linearly polarized radio emission

B-magnitude in microG

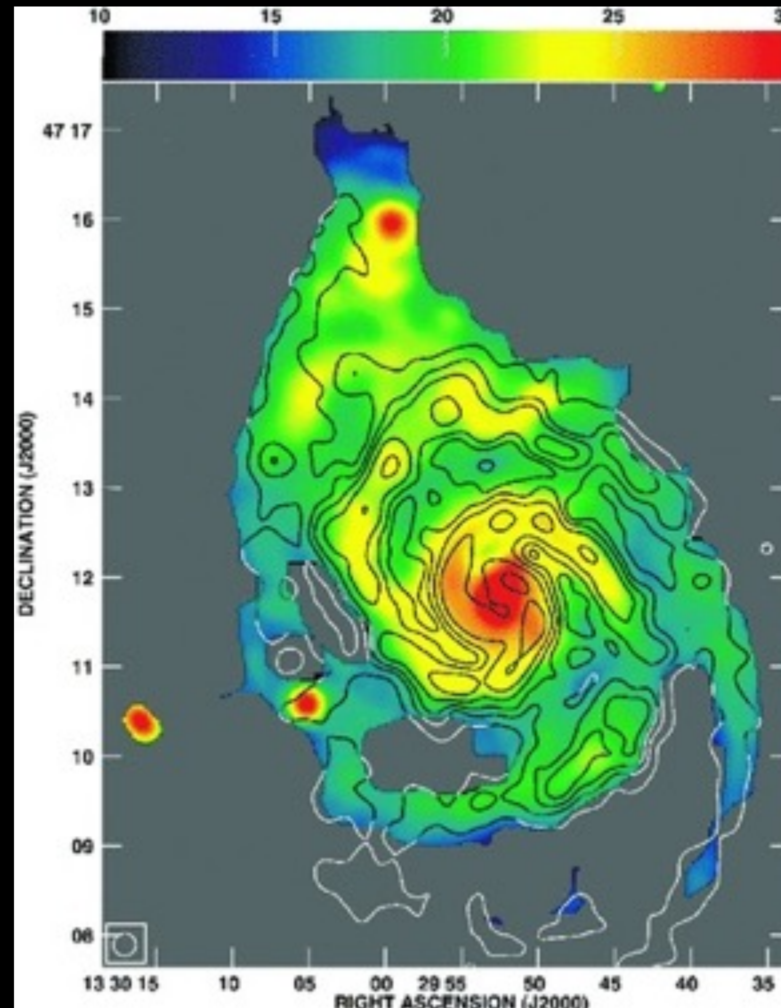

Field strength estimated by assuming energy equipartition with non-thermal synchrotron-emitting electrons

Fletcher+11

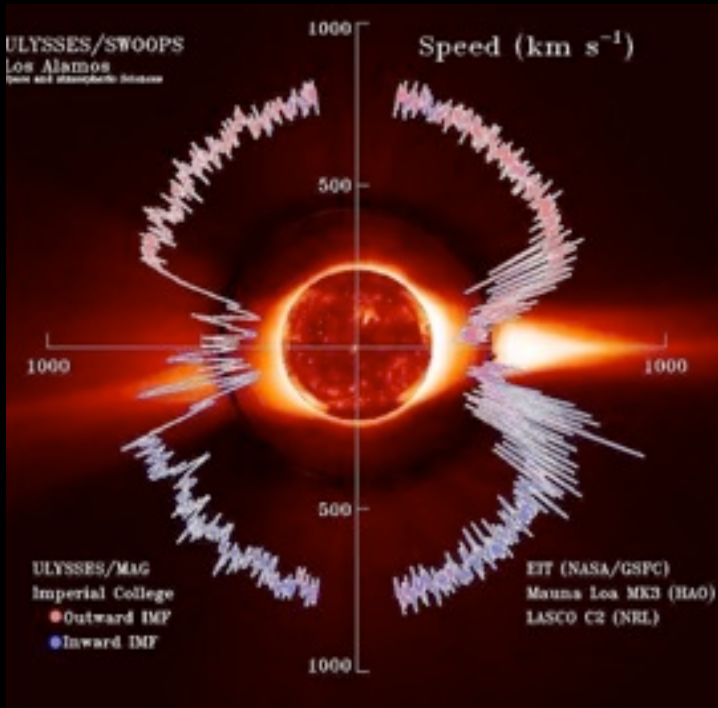

We suppose that the field at the coronal base has an energy density greater than the thermal energy density, so that an initially subsonic flow will follow the field-lines. Gas starting at sufficiently low latitudes will reach the equator at points not too far from the star, where the magnetic energy density is still larger than the thermal. Even if there were no hot gas outside the region defined by the loop ABA' in Fig. 1, exerting an inward pressure, the gas within ABA' would reach equilibrium: a very slight denting of the field-lines would generate the discontinuity in the magnetic pressure $\mathbf{H}^2/8\pi$ that would balance the discontinuity in thermal pressure. But gas expanding along field lines such as EC cannot reach such a state of hydrostatic equilibrium. Before it has expanded far enough to reach the equator, it will find that its pressure exceeds the magnetic pressure, so that it will cease to flow along prescribed, nearly dipole field-lines: instead it will expand more-or-less radially, dragging the field with it.

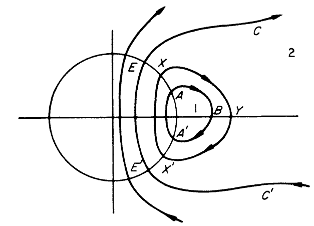

Fig. 1

Mestel 65

The picture we arrive at finally is as in Fig. 1. There is a dead zone (1) in which the closed, approximately dipolar field-loops hold in the gas and keep it rotating with the star's angular velocity Ω_s. The density field ρ along each field-line is given by the component of hydrostatic support along the field: assuming isothermality with sound speed a,

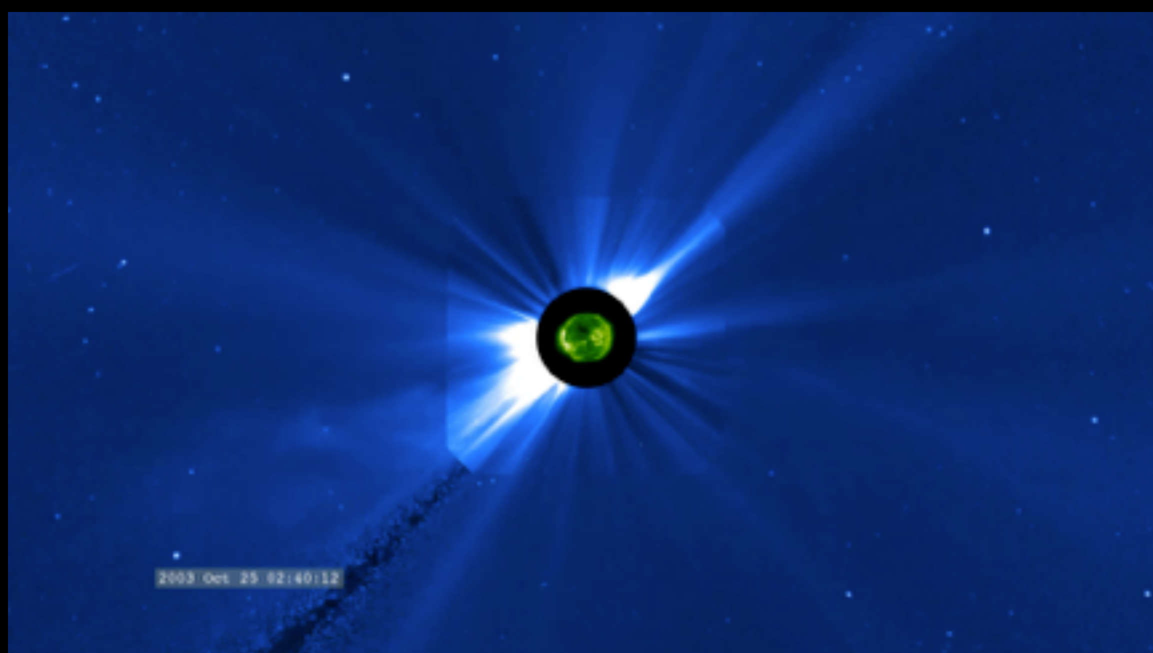

“Pulsar in a Box”

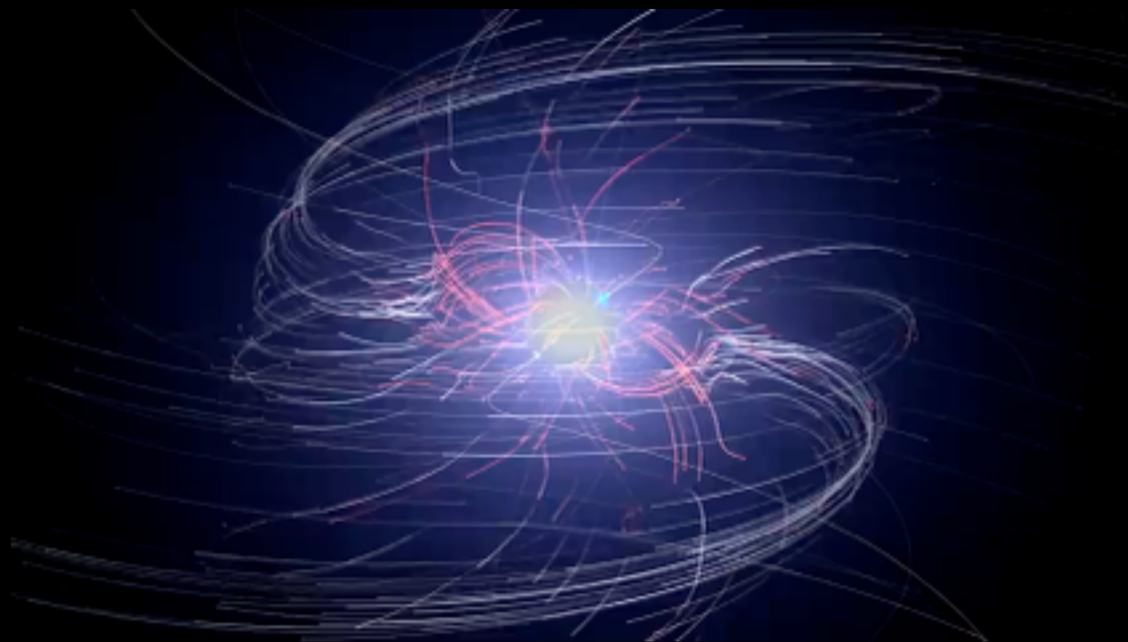

“Pulsar wind nebula” in Crab Nebula

1 pc

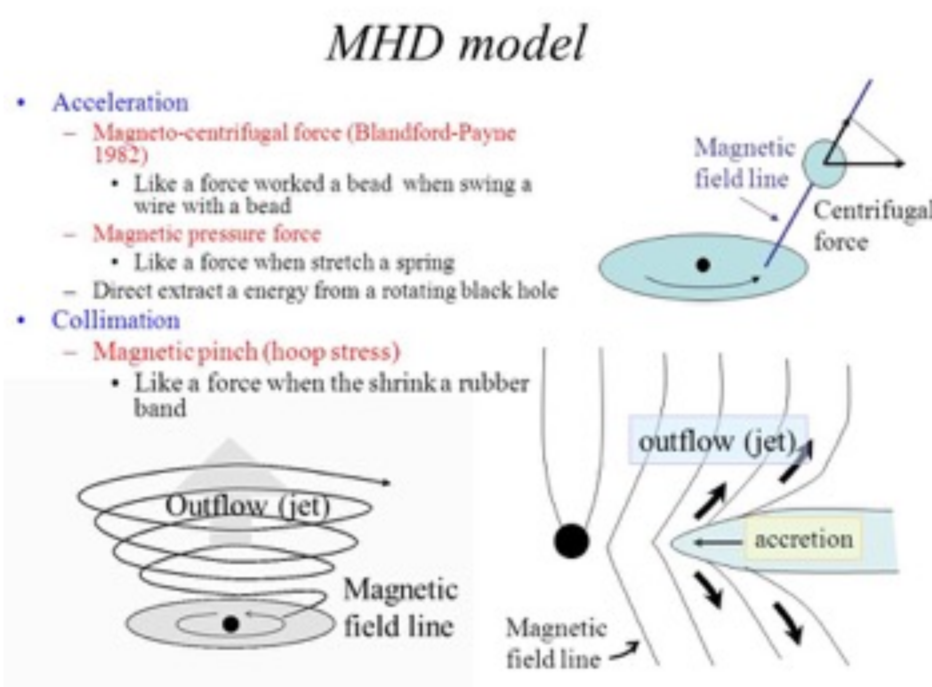

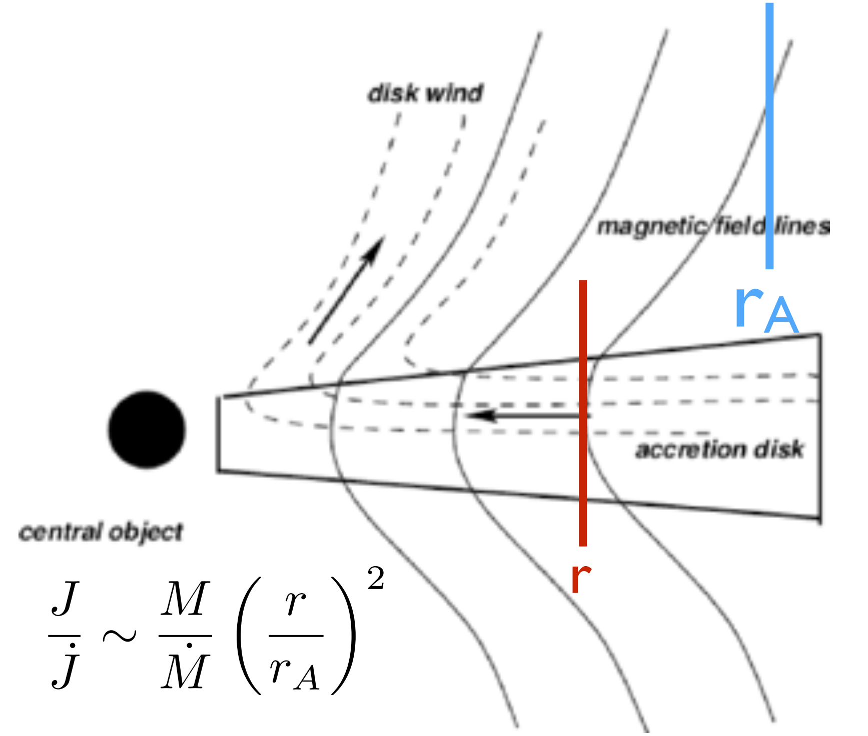

$$\frac{J}{\dot{J}} \sim \frac{M}{\dot{M}} \left(\frac{r}{r_A}\right)^2$$

Blandford & Payne 82

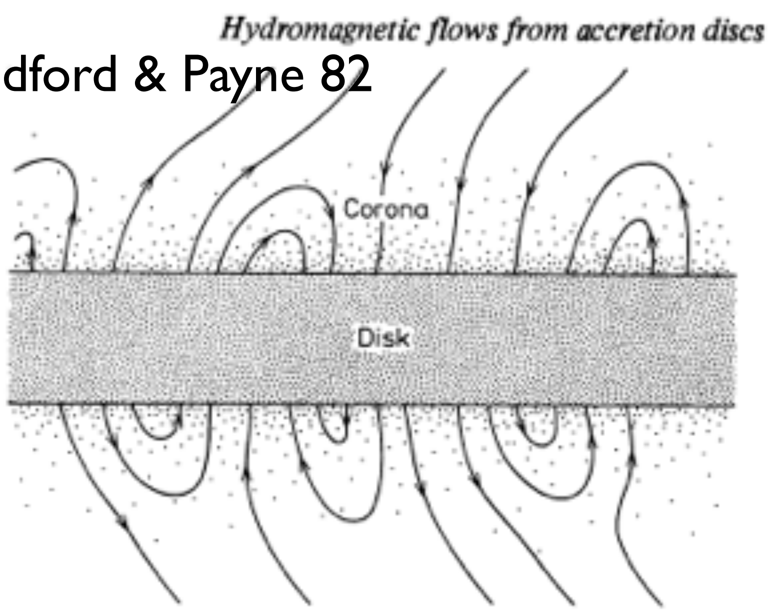

Figure 5. A schematic representation of a possible field geometry close to the disc.

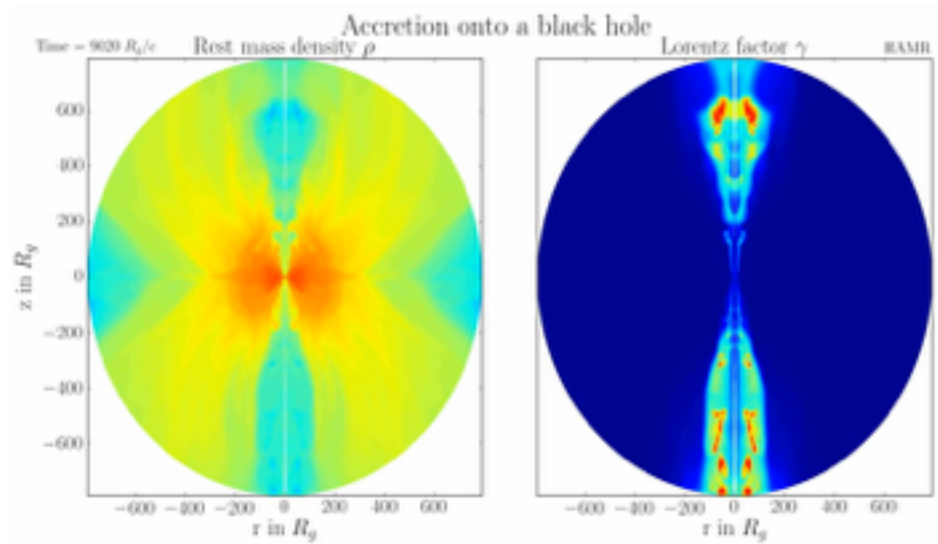

Hesp, Liska, Tchekhovskoy

flux freezing

$$d\Phi/dt = 0$$

$$\Updownarrow$$

fluid parcel tied to field line

$$d(\vec{B}/\rho)/dt = (\vec{B}/\rho \cdot \nabla)\vec{u}$$

$$\neq$$

fluid parcel travels ALONG field line

$$\vec{u} \parallel \vec{B} \quad \longleftarrow \text{actually false}$$

from Ferraro's law derivation (assumes $\partial/\partial t = 0$!)

$$\frac{u_z}{u_r} = \frac{B_z}{B_r}$$

"bead on a steady poloidal wire"

Parker spiral = steady, but not poloidal wires!

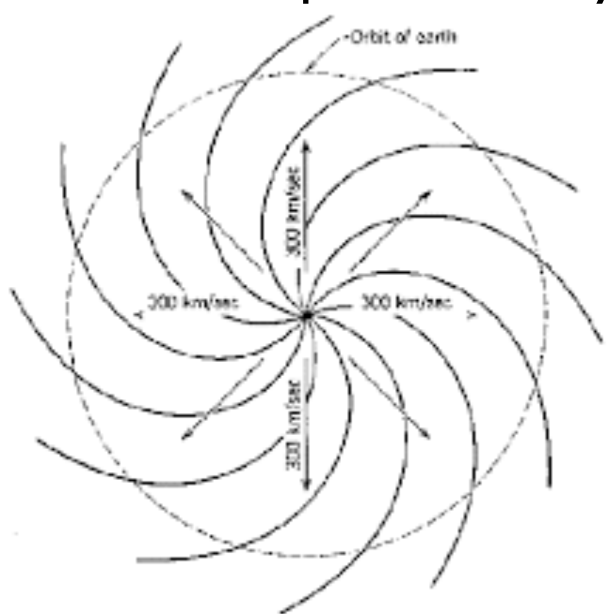

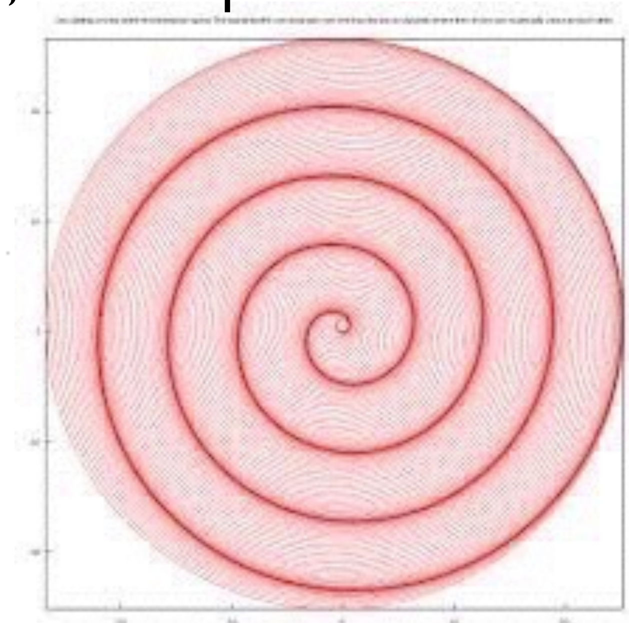

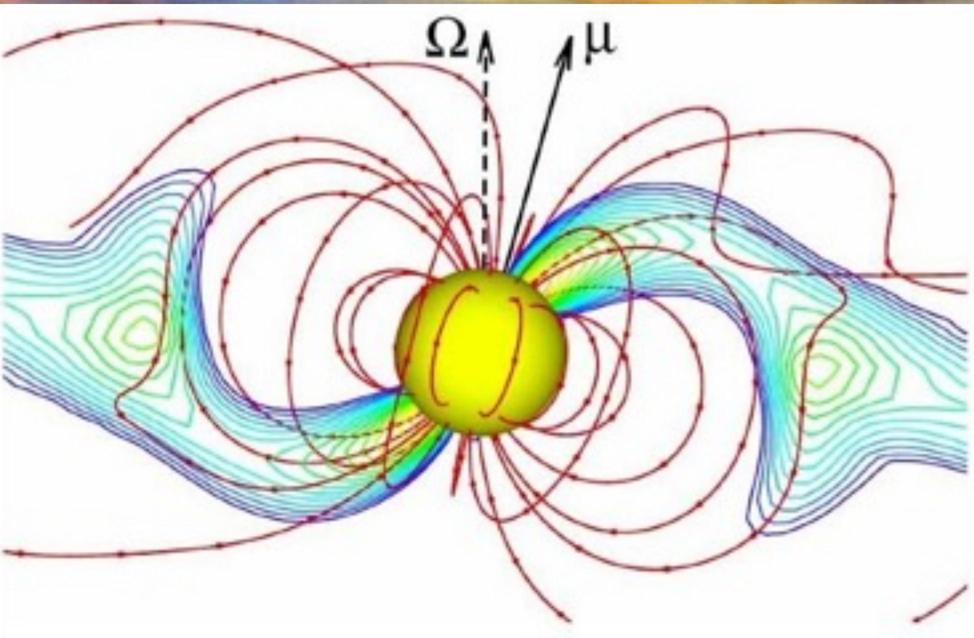
Ω
μ

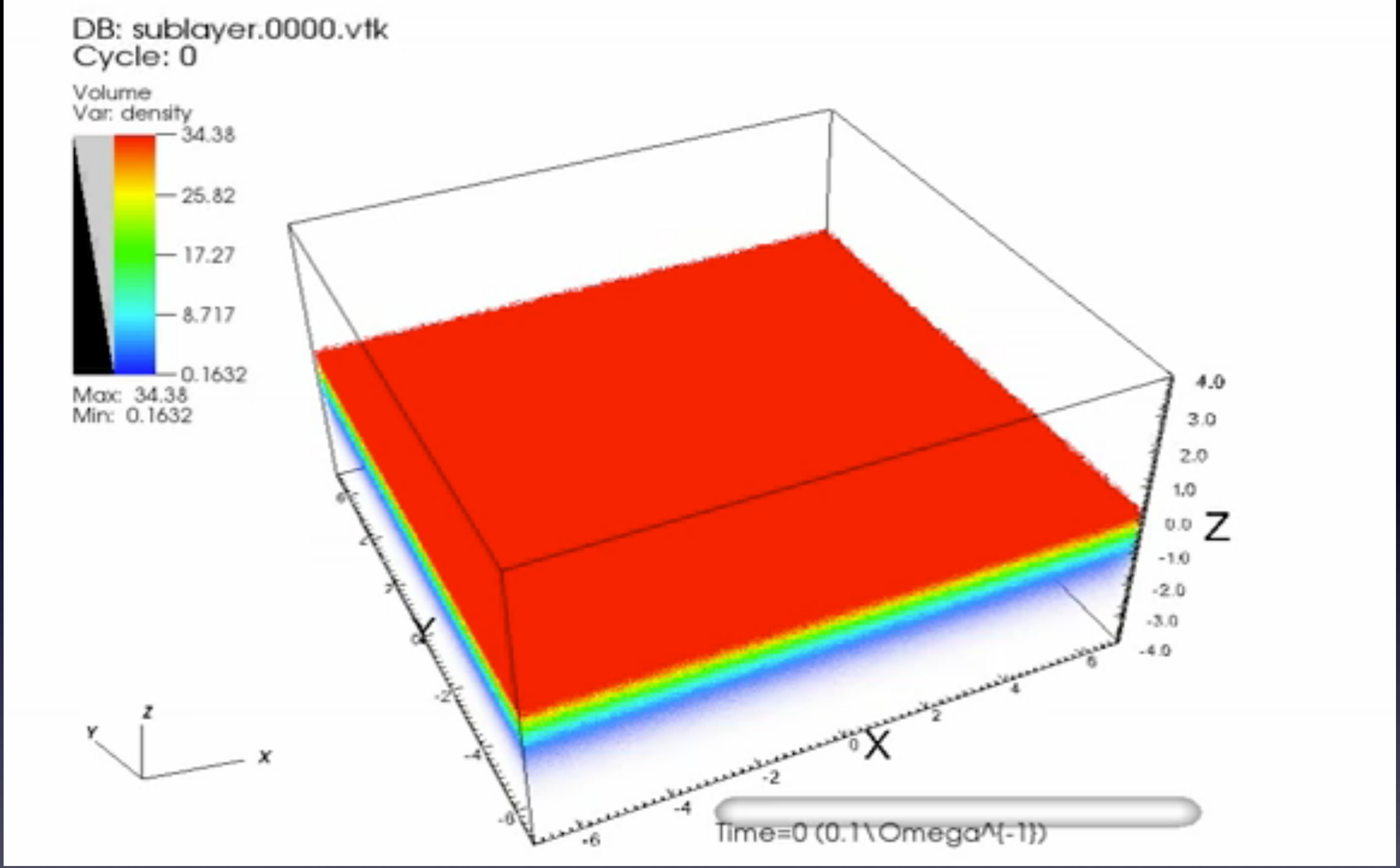

Q ~ 1 and fast cooling $t_{\rm cool} < t_{\rm shear} \sim 1/\Omega$

gravitational collapse

Shi & Chiang 13

Gravito-turbulence

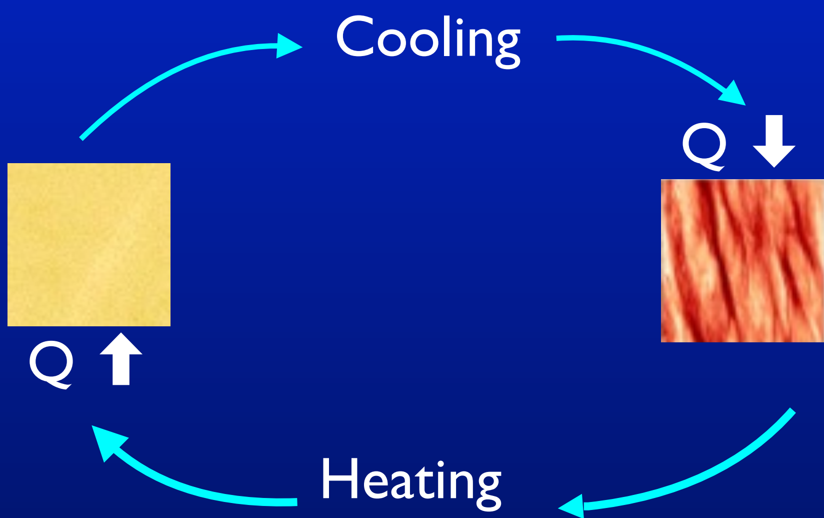

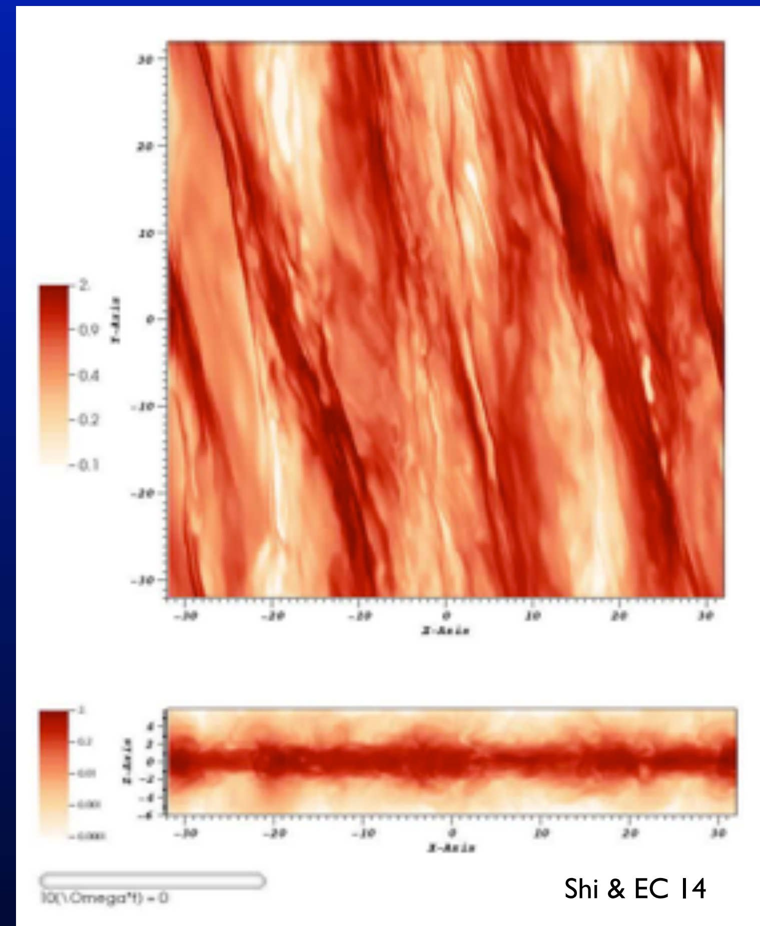

$$Q = \frac{c_s \kappa}{\pi G \Sigma} \sim 1$$

and slow cooling

$$t_{\rm cool} > t_{\rm shear} \sim 1/\Omega$$

Magneto-rotational instability (MRI) / Balbus & Hawley 91, Hawley & Balbus 91

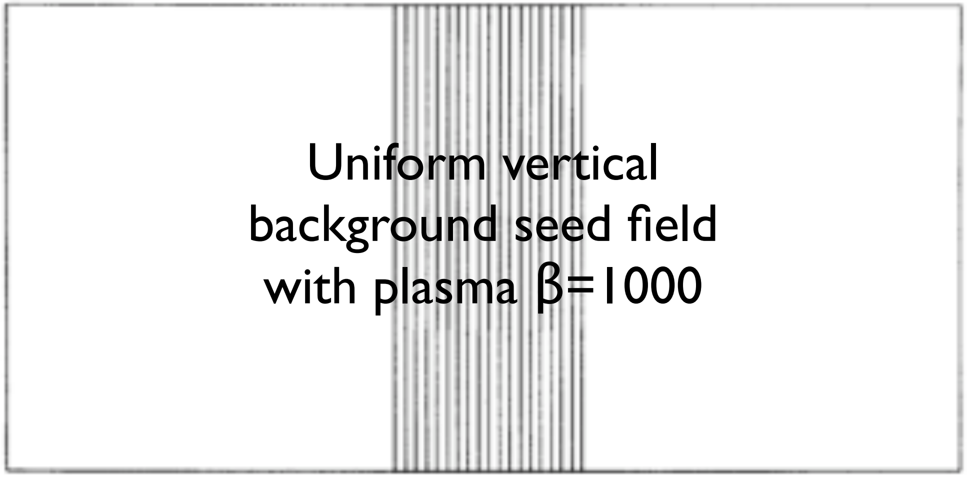

FIG. 3a

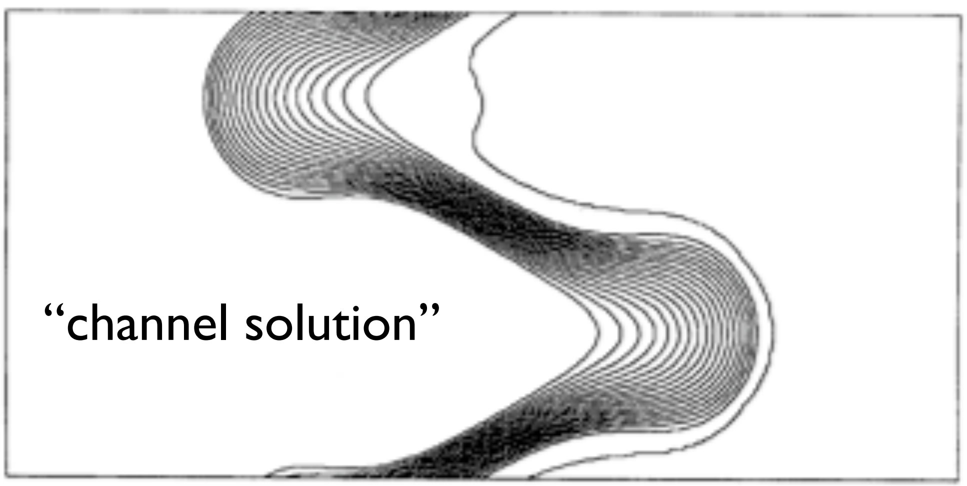

FIG. 3b

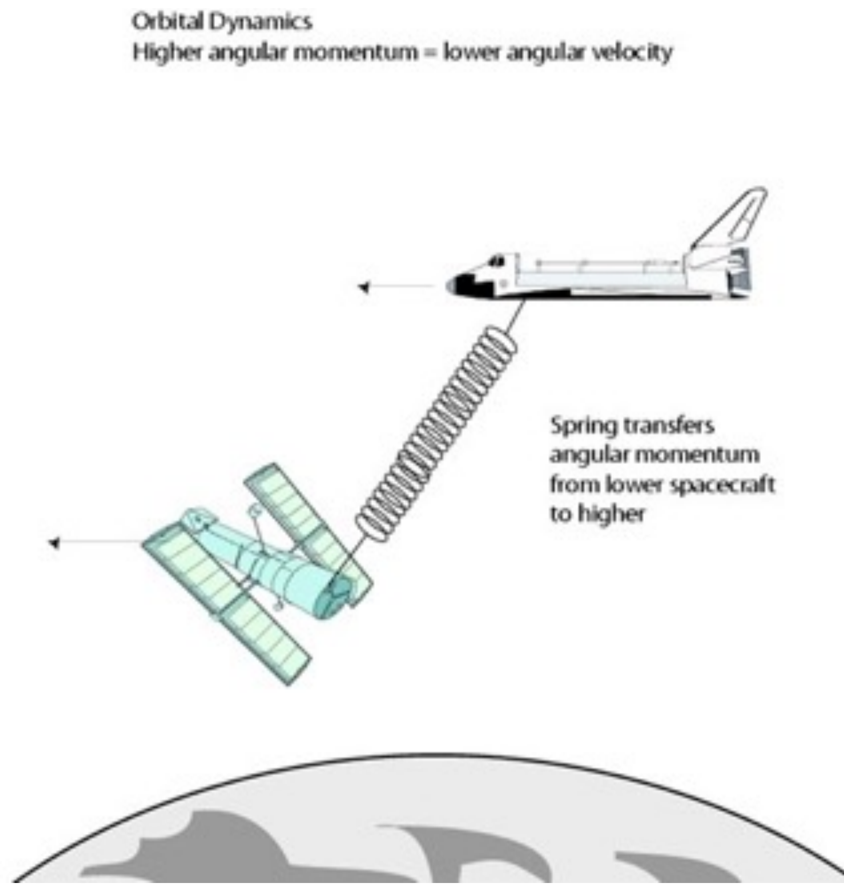

Hawley 2000

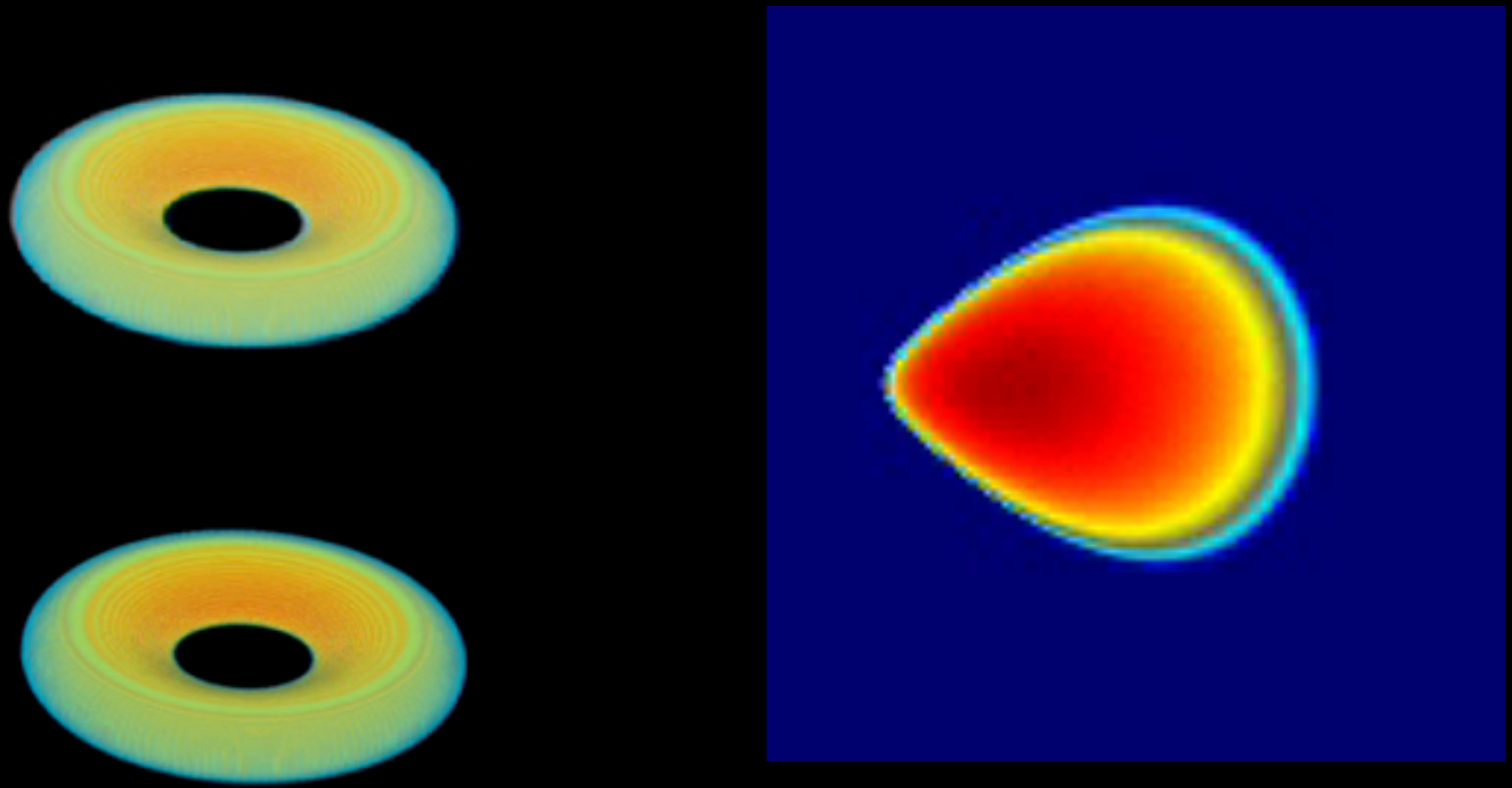

MRI in 3-D

Colors denote log density

Initially poloidal field

Hawley, Gammie, & Balbus 95

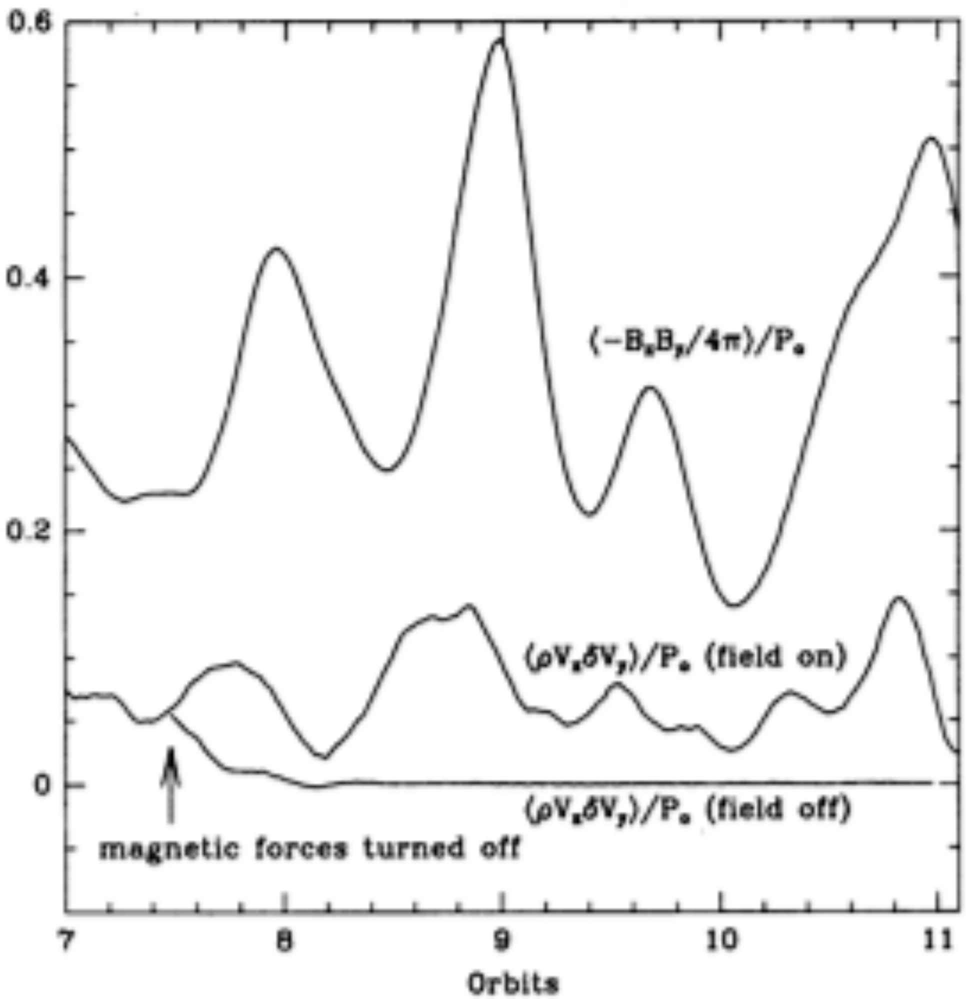

FIG. 7.—The Maxwell and Reynolds stresses in the fiducial run Z4 compared with the Reynolds stress seen in a purely hydrodynamical simulation that is initialized with data from model Z4 at time $t = 7.5$. Without magnetic fields the net Reynolds stress vanishes within one orbit. The time series are boxcar smoothed on a timescale of 0.25 orbits.

Uniform vertical background seed field with plasma β=400

Bai & Stone 13a

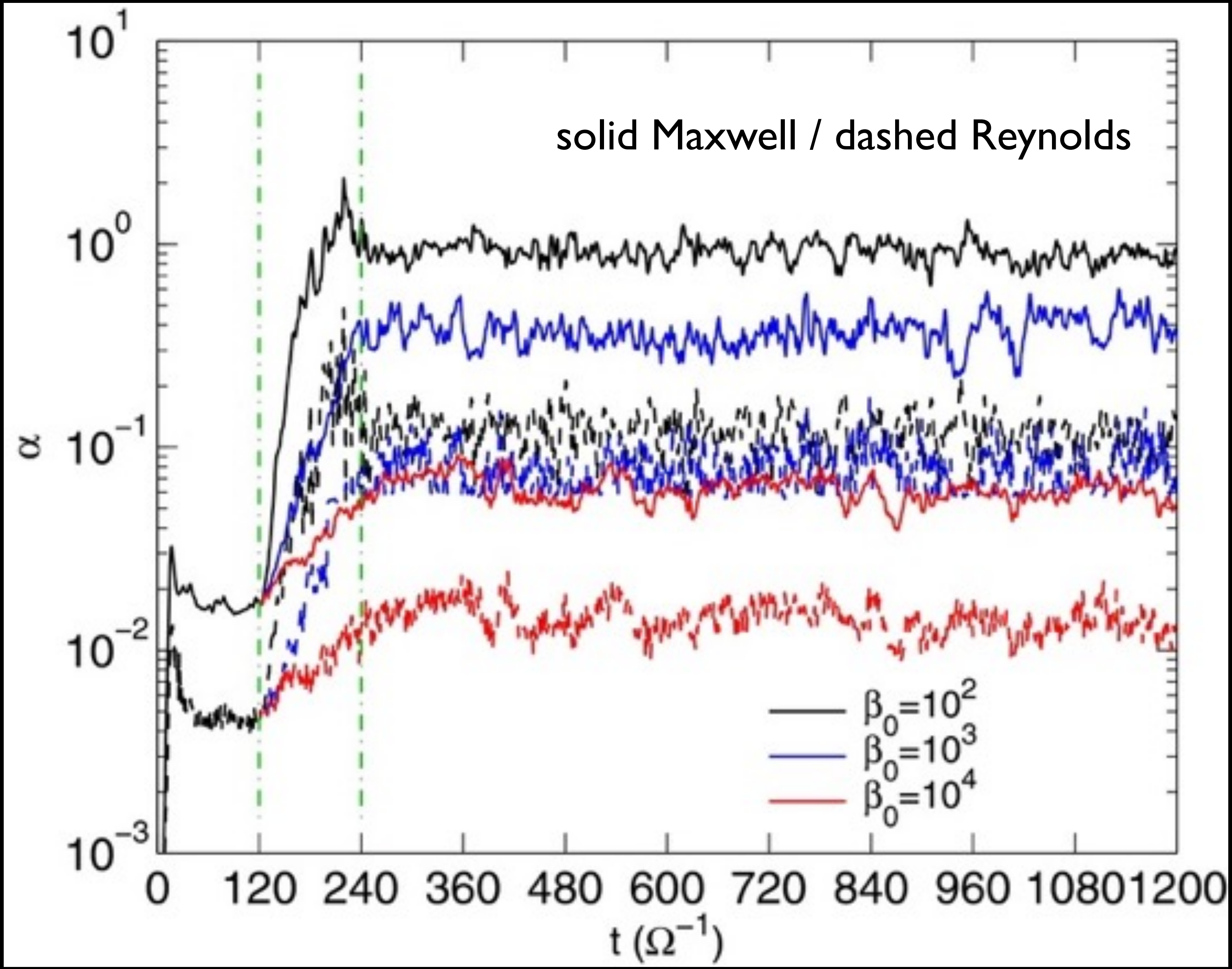

uniform net vertical B_0

Bai & Stone 13a

MRI as dynamo: Generation of large and cyclical toroidal B_φ

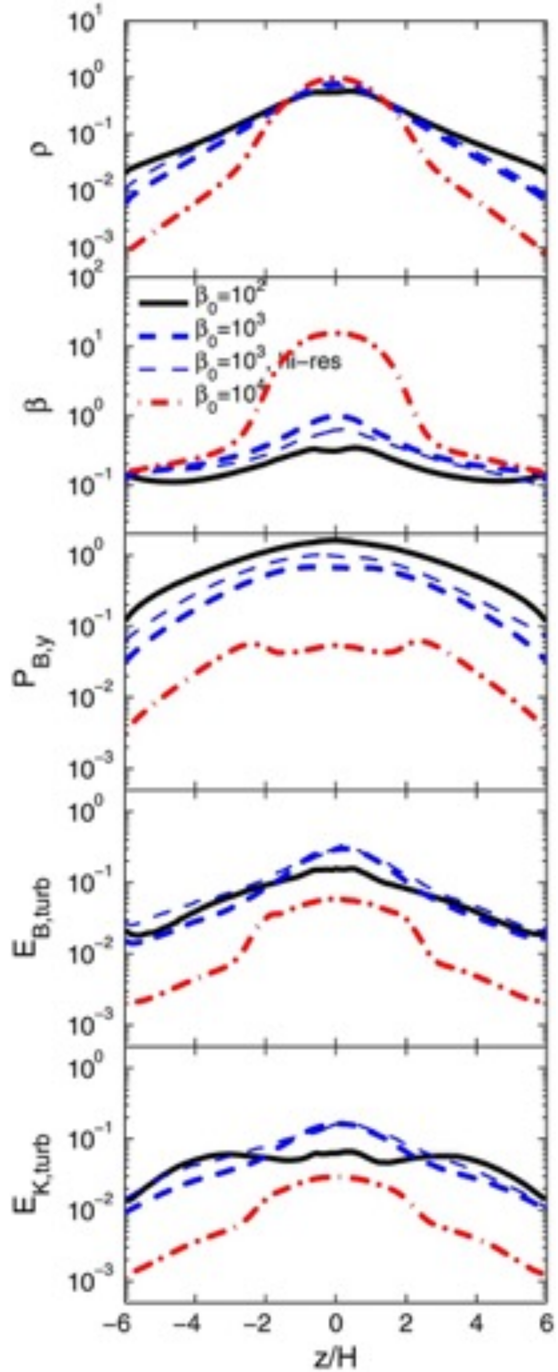

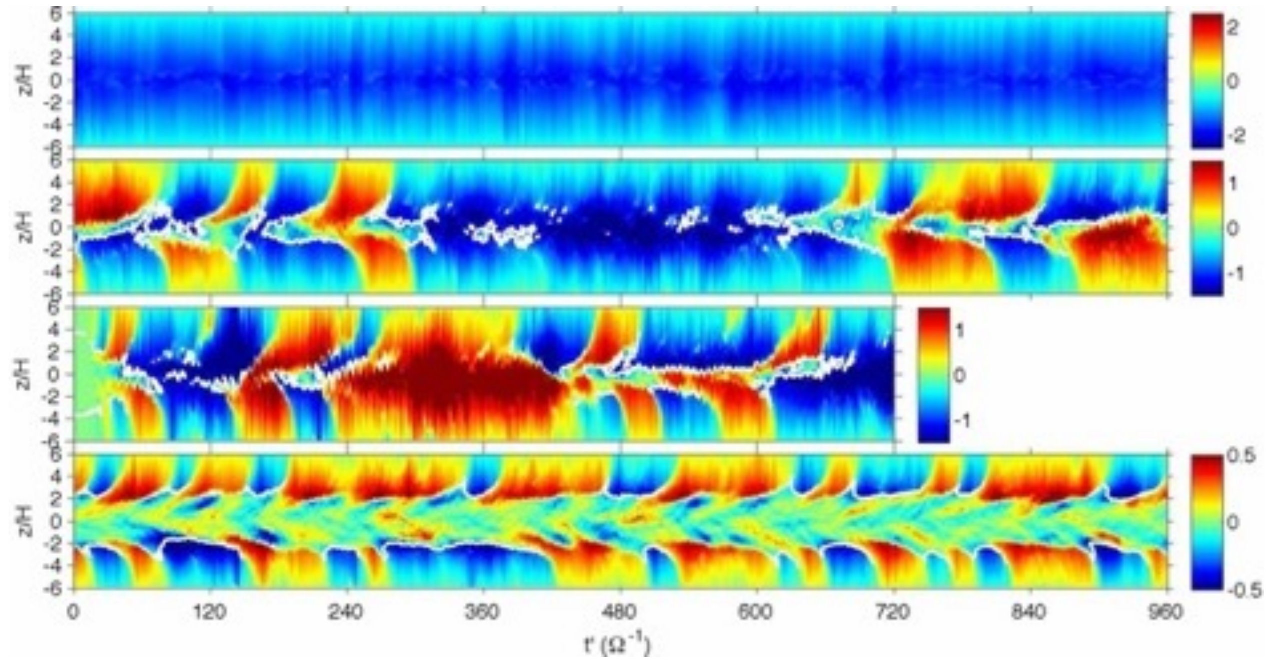

"magnetic tower" outflows

$$\frac{1}{2}\rho\Omega v_R \approx \frac{B_z}{4\pi}\frac{dB_\phi}{dz}$$

transports angular momentum
VERTICALLY
to drive RADIAL accretion

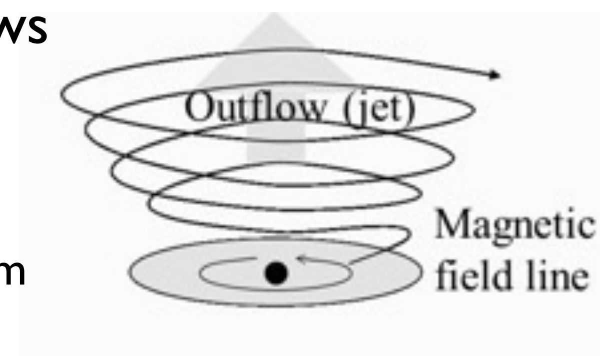

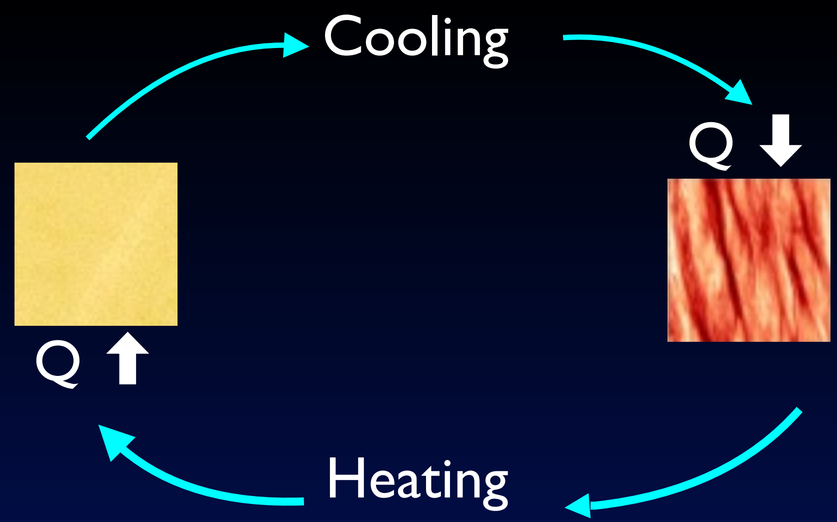

Gravito-turbulence

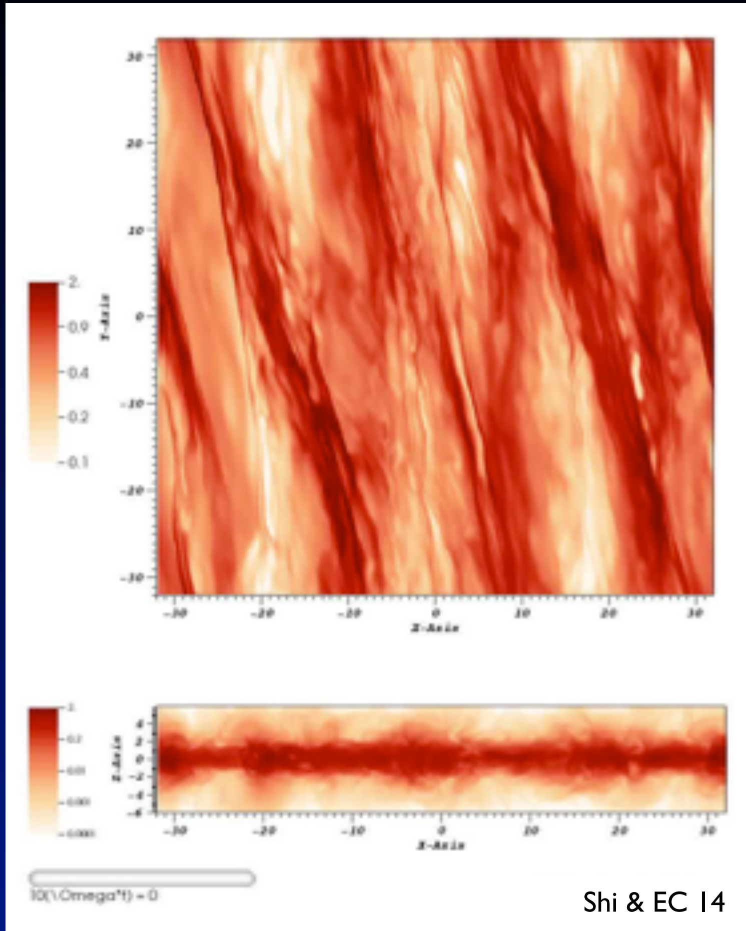

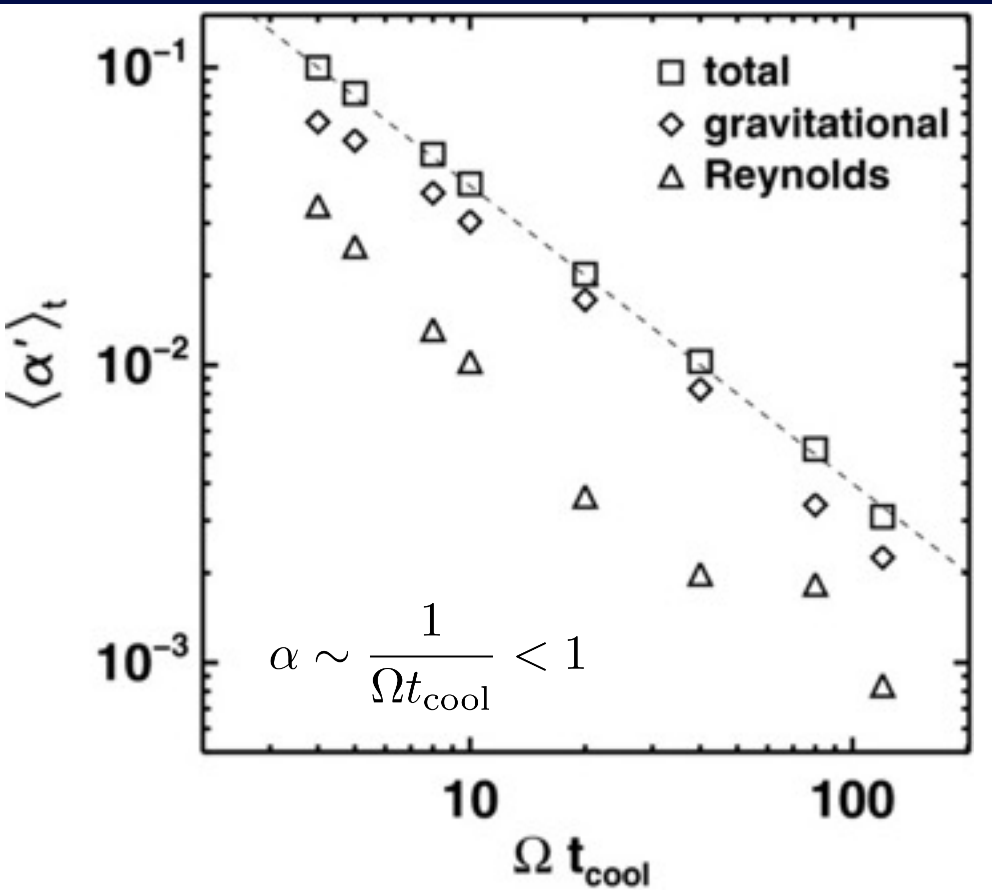

$$\alpha \equiv \frac{\langle w_{xy}\rangle_\rho}{\langle P\rangle_\rho} \equiv \frac{\langle g_x g_y/4\pi G + \rho v_x \delta v_y\rangle_\rho}{\langle P\rangle_\rho}$$

Self-gravity swing-amplifies perturbations into strong trailing spirals which transport angular momentum outward

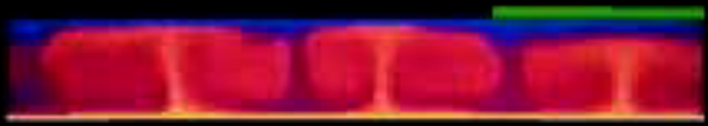

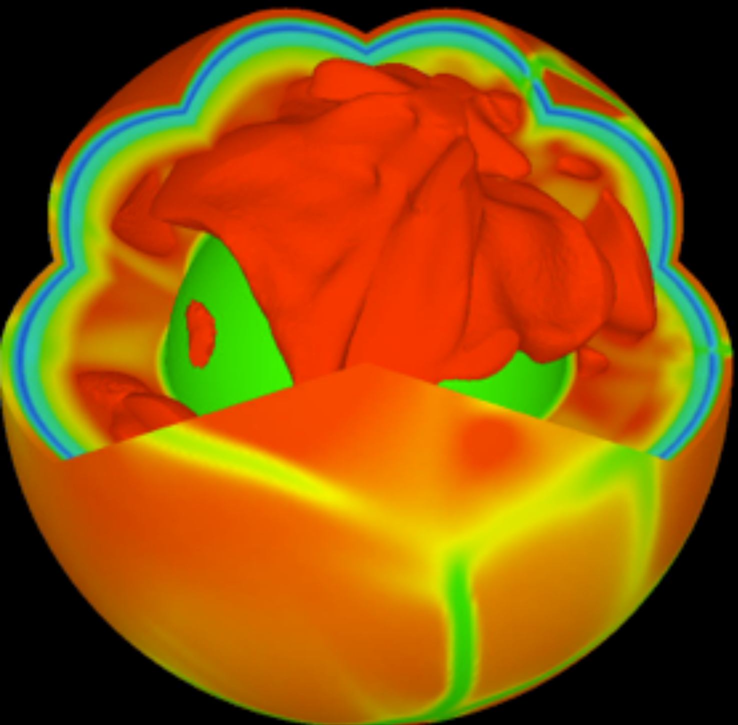

unstable

^

hydrostatic equilibrium

$$\omega^2_{\mathrm{Brunt-Vaisala}} = \left[\frac{1}{\gamma}\frac{\partial P}{\partial z} - \frac{\partial \rho}{\partial z}\right] g$$

$$= \frac{g}{\gamma}\frac{\partial s}{\partial z}$$

$\vec{g} = -g\hat{z}$

$P(z)$

$\rho(z)$

> 0 stable

< 0 unstable

$\therefore$ convection

Mantle convection

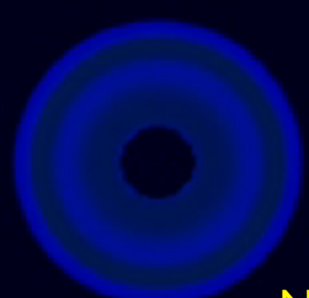

Neutrino-driven convection in supernovae

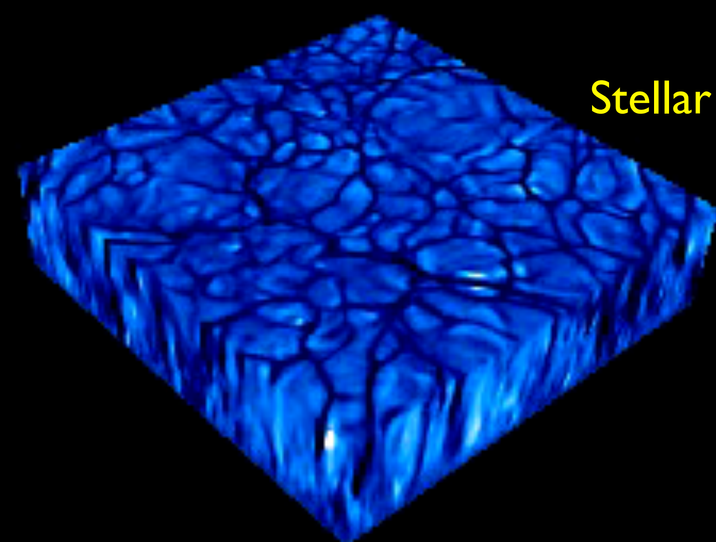

Stellar convection

Necessary (not sufficient) criterion for K-H instability in Cartesian shear flow:

Richardson $$Ri \equiv \frac{\omega^2_{\mathrm{Brunt-Vaisala}}}{(\partial u/\partial z)^2} < Ri_{\mathrm{crit}} = \frac{1}{4}$$ see Shu for heuristic derivation

Kelvin-Helmholtz (K-H) Instability

Cartesian shear, if too strong, can overturn an otherwise stably stratified atmosphere

for formal linear analysis, including analysis of contact discontinuity in ρ and v, see Chandrasekhar 61

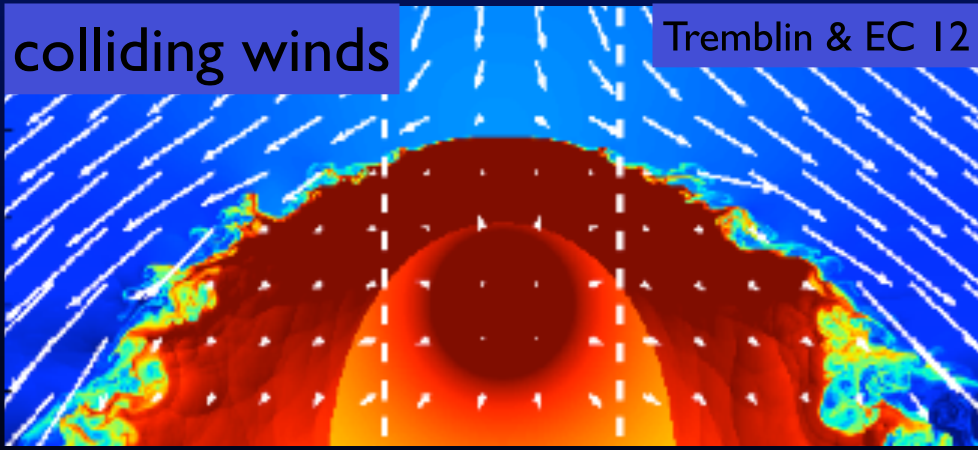

Turbulent Cascade

Big whorls have little whorls,
which feed on their velocity.
Little whorls have lesser whorls,
and so on to viscosity.

Lewis Fry Richardson (cf. Jonathan Swift)

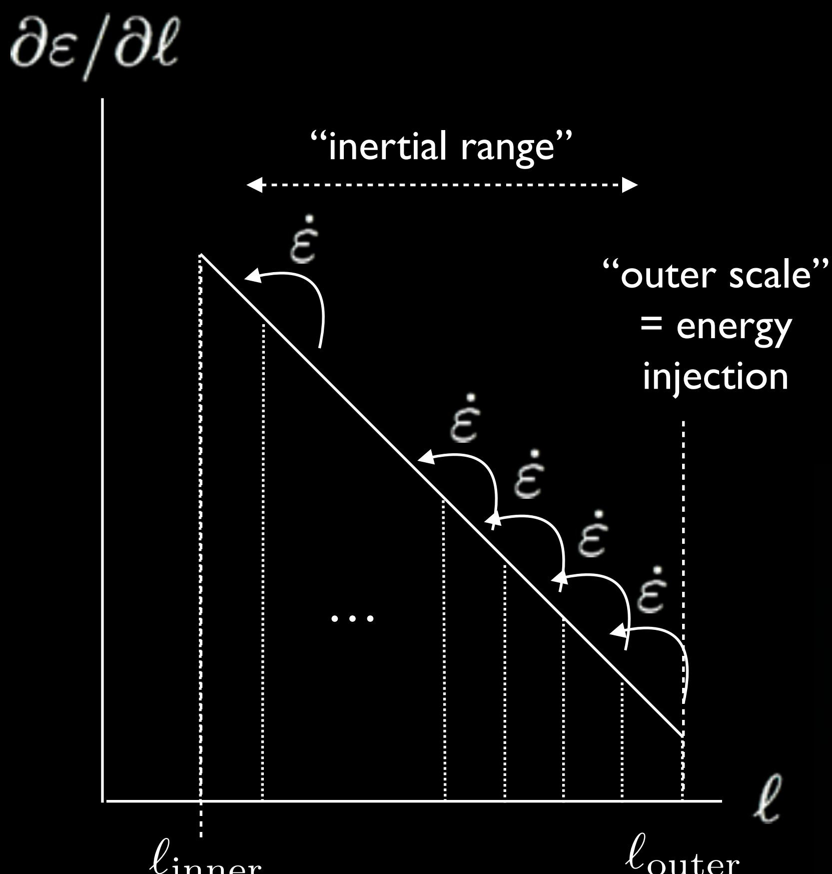

"inner scale"

= energy dissipation (energy goes into heat)